Chapter 7. Heating and Cooling Processes

Notes:

- *Most of the material presented in this chapter is taken from Stahler and Palla (2004), Chap. 7 and Appendix B.*

7.1 Cosmic Rays

We have already mentioned the fact that we need the presence of ions in molecular clouds to explain the abundance of most molecular species detected through observations. We could postulate that the needed ionization comes from stellar radiation emanating from either within or outside star-forming regions. But that would fail to account for the fact that ions exist deep inside the interior of molecular clouds devoid of (proto-) stars and their corresponding ionizing radiation. Something else is needed to explain the observations…

Gamma rays, mostly consisting of relativistic protons, with some heavier nuclei as well as electrons, provide the answer. As they penetrate the interstellar medium and molecular clouds, gamma rays interact with the constituents of the gas through the Coulomb and nuclear forces. In molecular clouds, the most probable outcome from the inelastic scattering of cosmic rays with H_2 results in the ionization of the latter. This reaction is represented with

$$p^+ + H_2 \rightarrow H_2^+ + e^- + p^+. \tag{7.1}$$

This production of pairs of oppositely charged particles is the main source of ionization in the interiors of molecular clouds. We already know that this ionization is essential for establishing ion-molecule chemical reactions, but it also leads to the **flux-freezing** phenomenon, where the magnetic field becomes tied (or coupled) to the gas and vice-versa. Furthermore, the release of the electron provides heating as it interacts with gas after its ejection.

The **rate of heat deposition per unit volume** $\Gamma_{CR}(H_2)$ can be expressed as

$$\Gamma_{CR}(H_2) = \varsigma(H_2) n_{H_2} \Delta E(H_2) \ \text{ erg cm}^{-3}\text{s}^{-1}, \tag{7.2}$$

where $\varsigma(H_2)$ is the **cosmic ray ionization rate** for a single H_2 molecule, n_{H_2} is the volume density of H_2, and $\Delta E(H_2)$ is the thermal energy added to the gas from an ionization event. Diverse processes must be taken into account when evaluating $\Delta E(H_2)$, but the most important one is the further dissociation of H_2 through interaction with the released electron through

$$e^- + H_2 \rightarrow H + H + e^-. \tag{7.3}$$

But summing up all the different processes a value of $\Delta E(\mathrm{H_2}) \simeq 7.0$ eV is obtained (with $1\ \mathrm{eV} = 1.602 \times 10^{-12}$ erg).

The same cosmic ray ionizing process takes place in diffuse clouds, but this time involving atomic instead of molecular hydrogen. This reaction is represented with

$$\mathrm{p^+ + H \rightarrow H^+ + e^- + p^+}. \tag{7.4}$$

The amount of heating resulting from this process can be expressed in a similar manner to the previous one involving $\mathrm{H_2}$

$$\Gamma_{\mathrm{CR}}(\mathrm{HI}) = \varsigma(\mathrm{HI}) n_{\mathrm{HI}} \Delta E(\mathrm{HI}) \ \ \mathrm{erg\ cm^{-3} s^{-1}}, \tag{7.5}$$

with like definitions for the different parameters. It is found that $\Delta E(\mathrm{HI}) \simeq 6.0$ eV .

There are several methods used to determine the cosmic ray ionization rates $\varsigma(\mathrm{H_2})$ and $\varsigma(\mathrm{HI})$, but most of them rely on our understanding of ion-molecule chemical networks and relevant observations. We will presently discuss one technique that was developed here at Western (Hezareh et al. 2008, ApJ, 684, 1221).

We consider the main creation and destruction networks for the $\mathrm{HCNH^+}$ and $\mathrm{HCO^+}$ molecular ions. That is, for the first species we have

$$\begin{aligned} \mathrm{H_3^+ + HCN(HNC) \rightarrow HCNH^+ + H_2} \\ \mathrm{HCO^+ + HCN(HNC) \rightarrow HCNH^+ + CO} \\ \mathrm{H_3O^+ + HCN(HNC) \rightarrow HCNH^+ + H_2O}, \end{aligned} \tag{7.6}$$

while for the latter we simply have

$$\mathrm{H_3^+ + CO \rightarrow HCO^+ + H_2}. \tag{7.7}$$

And both ion species are mainly destroyed through electron recombination with

$$\begin{aligned} \mathrm{HCNH^+ + e^-} &\rightarrow \mathrm{HCN + H} \\ &\rightarrow \mathrm{HNC + H} \\ &\rightarrow \mathrm{CN + H + H} \\ \mathrm{HCO^+ + e^-} &\rightarrow \mathrm{CO + H}. \end{aligned} \tag{7.8}$$

Assuming equilibrium between the creation and destruction rates these equations can be combined to obtain the following expressions for the electron and $\mathrm{H_3^+}$ densities

$$n(\mathrm{e}^-) = \left\{\left[n(\mathrm{HCN}) + n(\mathrm{HNC})\right]\cdot\left[n(\mathrm{H}_3^+)k_1 + n(\mathrm{HCO}^+)k_2 + n(\mathrm{H}_3\mathrm{O}^+)k_3\right]\right\} / n(\mathrm{HCNH}^+)k_5 \qquad (7.9)$$

$$n(\mathrm{H}_3^+) = \frac{n(\mathrm{HCO}^+)n(\mathrm{e}^-)k_6}{n(\mathrm{CO})k_4}.$$

This is a system of two equations and two unknown (i.e., $n(\mathrm{e}^-)$ and $n(\mathrm{H}_3^+)$) that can be readily solved as long as the abundances of all the other molecular species are known a priory (i.e., those of $\mathrm{HCN}, \mathrm{HNC}, \mathrm{HCO}^+, \mathrm{H_3O}^+, \mathrm{HCNH}^+$, and CO). Fortunately, these can be determined observationally with the methods covered in Chapter 6. The **rate coefficients** k_i in equations (7.9) are determined experimentally and are $\sim 10^{-8}(T/300\ \mathrm{K})^{-0.5}\ \mathrm{cm^3\,s^{-1}}$ for i.e., $i = 1, 2,$ and 3, $\sim 10^{-7}(T/300\ \mathrm{K})^{-0.7}\ \mathrm{cm^3\,s^{-1}}$ for $i = 5$ and 6, and $\sim 10^{-9}\ \mathrm{cm^3\,s^{-1}}$ for k_4. The determination of the electron and H_3^+ abundances through equations (7.9) is an important byproduct of our quest for the evaluation of the cosmic ray ionization rate, which can be accomplished by finally considering the main routes for the creation and destruction of H_3^+

$$\begin{aligned} \mathrm{H_2} + \mathrm{CR} &\rightarrow \mathrm{H_2^+} + \mathrm{e^-} \\ \mathrm{H_2^+} + \mathrm{H_2} &\rightarrow \mathrm{H_3^+} + \mathrm{H} \end{aligned} \qquad (7.10)$$

and

$$\begin{aligned} \mathrm{H_3^+} + \mathrm{CO} &\rightarrow \mathrm{HCO^+} + \mathrm{H_2} \\ \mathrm{H_3^+} + \mathrm{e^-} &\rightarrow \mathrm{H_2} + \mathrm{H} \\ &\rightarrow \mathrm{H} + \mathrm{H} + \mathrm{H}. \end{aligned} \qquad (7.11)$$

The reaction between H_2 and H_2^+ proceeds very rapidly and is limited by the abundance of H_2^+, the creation of H_3^+ is therefore governed by the ionization of H_2 from cosmic rays. Again assuming equilibrium for the formation and destruction of H_3^+ we get

$$\varsigma(\mathrm{H_2}) = \frac{n(\mathrm{H}_3^+)n(\mathrm{CO})k_4 + n(\mathrm{H}_3^+)n(\mathrm{e}^-)k_{11}}{n(\mathrm{H_2})}. \qquad (7.12)$$

where $k_{11} \sim 10^{-7}(T/300\ \mathrm{K})^{-0.5}\ \mathrm{cm^3\,s^{-1}}$ and the density of H_2 is determined using that of CO obtained from observations (see Chapter 6).

Estimates of the cosmic ray ionization rate can vary significantly as a function of the type of sources studied and the techniques used. A value of $\varsigma(\mathrm{H_2}) = 3\times 10^{-17}\ \mathrm{s^{-1}}$ for this

parameter is frequently used in the literature. The column density for H_3^+ is on the order of $10^{14}\,\mathrm{cm}^{-2}$. As we will see in Chapter 8, the ionization fraction $\left[e^-\right] \equiv n(e^-)/n(\mathrm{HI})$ will vary with the gas density, but values of $10^{-7} - 10^{-8}$ are representative (we will revisit the determination of ionization fraction in the next chapter). Using equation (7.2) we then find that

$$\Gamma_{\mathrm{CR}}(H_2) = 2\times10^{-13}\left(\frac{n_{H_2}}{10^3\,\mathrm{cm}^{-3}}\right)\ \mathrm{eV\ cm^{-3}s^{-1}}. \tag{7.13}$$

Theoretical considerations comparing the ionization rates of H_2 and HI show that

$$\varsigma(\mathrm{HI}) = 2\times10^{-17}\,\mathrm{s}^{-1} \tag{7.14}$$

and

$$\Gamma_{\mathrm{CR}}(\mathrm{HI}) = 1\times10^{-13}\left(\frac{n_{\mathrm{HI}}}{10^3\ \mathrm{cm}^{-3}}\right)\ \mathrm{eV\ cm^{-3}s^{-1}}, \tag{7.15}$$

which implies that the cosmic ray heating rate is the same for atomic and molecular gases.

7.2 Interstellar Radiation

Gamma rays do not constitute the only radiation field filling up the interstellar space, nor do they provide the sole source of heating and ionization in the interiors of molecular clouds. Interstellar radiation can also serve as a significant source of energy that must be taken into when considering the thermal balance in star-forming regions.

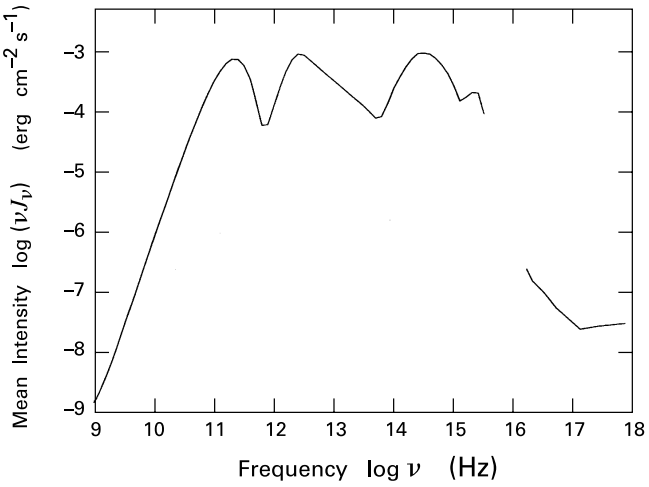

Figure 7.1 - Mean intensity of the interstellar radiation in the solar neighbourhood.

Figure 7.1 shows a plot of the mean intensity of the interstellar radiation in the solar neighbourhood; please note that νJ_ν is actually shown and not J_ν. We can see from this graph that although interstellar radiation peaks at millimetre wavelengths (i.e., $\log\nu = 11.3$), there are two additional maxima at far-infrared ($\log\nu = 12.4$) and optical ($\log\nu = 14.5$) wavelengths. These three peaks correspond to radiation due to the cosmic microwave background (CMB; $T = 2.74$ K), starlight-irradiated dust grains, and background light from field stars (with an equivalent blackbody peak at a temperature of $T \simeq 5{,}400$ K; see eq. (2.32) on Chapter 2), respectively. Only the CMB and optical radiation fields represent significant sources of heating in molecular clouds. This is because CMB radiation at millimetre wavelengths is likely to excite the lowest rotational transitions of abundant molecules such as CO (e.g., the $^{12}\mathrm{C}^{16}\mathrm{O}(J = 1 \rightarrow 0)$ happens at approximately 115 GHz or 2.6 mm), and radiation in the optical range will tend to be heavily absorbed by dust grains. On the other hand, the gas in molecular clouds is mostly transparent to radiation at far-infrared wavelengths since abundant molecular species (again mostly CO) lack strong transitions in that range.

It is interesting to compare the peak intensity of a blackbody at a temperature of 5,400 K (i.e., $\nu B_\nu \simeq 10^{10}\,\mathrm{erg\,cm^{-2}s^{-1}sr^{-1}}$) to that of the interstellar radiation field in the corresponding wavelength range (i.e., $\nu J_\nu \simeq 10^{-3}\,\mathrm{erg\,cm^{-2}s^{-1}sr^{-1}}$). This leads to the definition of a **dilution factor** $W = 10^{-13}$, which represents the approximate fractional solid angle covered by field stars on the sky. Likewise, the secondary peak seen in the ultraviolet at $\log\nu = 15.3$ in Figure 7.1 has a blackbody-equivalent temperature $T = 3.4\times10^4\,\mathrm{K}$, corresponding approximately to a B0 spectral type star with a dilution factor $W = 10^{-17}$. The **UV flux enhancement factor** $G_\circ$ of a given radiation field, e.g., from a massive star, is defined as the ratio of that field's UV flux to that of the interstellar radiation field.

7.2.1 **Carbon Ionization**

Carbon is the most abundant atom after hydrogen, having a relative abundance of $n_\mathrm{C}/n_\mathrm{H} = 3\times10^{-4}$. Although most photons from the interstellar radiation field are not energetic enough to ionize HI at 13.6 eV, neutral carbon (or CI) can be significantly ionized at 11.2 eV. This will liberate electrons that will deposit their excess kinetic energy resulting from the ionizing process through collisions with neighbouring atoms (or molecules) and heat the ambient gas. This reaction is represented by

$$\mathrm{C} + h\nu \rightarrow \mathrm{C}^+ + \mathrm{e}^-, \tag{7.16}$$

and the rate of heat deposition per unit volume is expressed similarly as for the cosmic ray ionization of (atomic or molecular) hydrogen with

$$\Gamma_\mathrm{CR}(\mathrm{CI}) = \varsigma(\mathrm{CI})\, n_\mathrm{CI}\, \Delta E(\mathrm{CI}) \ \ \mathrm{erg\,cm^{-3}s^{-1}}. \tag{7.17}$$

Accordingly, $\varsigma(\mathrm{CI})$ is the ionization rate for a single CI molecule, n_{CI} is the volume density of CI, and $\Delta E(\mathrm{CI})$ is the average energy deposition from the colliding electron. It is found that $\varsigma(\mathrm{CI}) = 10^{-10}\,\mathrm{s}^{-1}$ and $\Delta E(\mathrm{CI}) = 1\ \mathrm{eV}$, and therefore

$$\Gamma_{\mathrm{CI}} = 4\times 10^{-11}\left(\frac{n_{\mathrm{H}}}{10^3\ \mathrm{cm}^{-3}}\right)\ \mathrm{eV\ cm^{-3}s^{-1}}, \tag{7.18}$$

assuming that atomic carbon is mostly neutral. For cases that a non-negligible fraction of carbon is ionized, then Γ_{CI} must be reduced accordingly.

7.2.2 **Photoelectric Heating (Ionization of Grains)**

Electrons within dust grains can also be ejected through the photoelectric effect. That is, photons in the UV range have enough energy to ionize dust grains. The photons actually dislodge the electrons from about 10 nm inside the surface of grains; the electrons that do escape (most of them do not) will leave the grain with an excess of approximately $1\ \mathrm{eV}$. This implies a net energy conversion $\varepsilon_{\mathrm{PE}} \simeq 0.01$ when we consider the typical 10 eV energy of the incident ionizing photon.

To calculate the rate of heat deposited per unit volume we assume that the specific intensity is isotropic, and therefore the mean intensity $J_\nu = I_\nu$, and that the dust grains are (very approximately) spherical. To simplify calculations, we first consider the energy crossing the surface of the grain by an incident radiation that is uniform and unidirectional. In other words, let us define a constant intensity $I'_\nu\left(=J_\nu\right)$ that is directed along, say, $\mathbf{e}_z$. Thus the amount of energy per unit frequency and time crossing one hemisphere (i.e., the one facing the incident radiation) of the grain of radius R is

$$\begin{aligned} E'_\nu &= 2\pi R^2 I'_\nu \int_0^{\pi/2} \cos(\theta)\sin(\theta)\,d\theta \\ &= \pi R^2 I'_\nu, \end{aligned} \tag{7.19}$$

where θ is the polar angle between the normal of the surface and $\mathbf{e}_z$. However, we must multiply this value by 4π to get the total energy flux through the surface of the grain when the intensity is isotropic. This is because the value calculated in equation (7.19) must now be added for all incoming direction over the sphere. We then have that the total energy flux per unit frequency and volume for a grain density of n_{d} is

$$\begin{aligned} u_\nu &= n_{\mathrm{d}} 4\pi^2 R^2 J_\nu \\ &= 4\pi n_{\mathrm{d}} \sigma_{\mathrm{d}} J_\nu, \end{aligned} \tag{7.20}$$

where $\sigma_{\mathrm{d}} = \pi R^2$ is the cross-section of a dust grain. It therefore follows that the rate of heat deposition per unit volume (due to photoelectric heating) is

$$\Gamma_{\rm PE} = 4\pi n_{\rm d}\sigma_{\rm d}\varepsilon_{\rm PE}\int_{\rm FUV} J_\nu\, d\nu, \tag{7.21}$$

with the frequency integration is performed over the (potentially) ionizing band, i.e., in the far-ultraviolet, as indicated. We saw in Chapter 2 that the total geometric cross-section per hydrogen atom is

$$\begin{aligned}\Sigma_{\rm d} &\equiv \frac{n_{\rm d}\sigma_{\rm d}}{n_{\rm H}} \\ &= 1.1\times10^{-21}\ {\rm cm}^2,\end{aligned} \tag{7.22}$$

while it is determined from observations that the so-called **Habing flux** is

$$4\pi\int_{\rm FUV} J_\nu\, d\nu \simeq 1.6\times10^{-3}\ {\rm erg\ cm^{-2}s^{-1}}. \tag{7.23}$$

Performing a similar analysis for small grains, i.e., smaller and more abundant than the $\sim 0.1\ \mu$m grains considered so far, then we find that $\Gamma_{\rm PE}$ is elevated to

$$\Gamma_{\rm PE} = 3\times10^{-11}\left(\frac{n_{\rm H}}{10^3\ {\rm cm^{-3}}}\right)\ {\rm eV\ cm^{-3}s^{-1}}, \tag{7.24}$$

since smaller grains are more likely to eject electrons.

Finally, we note that although electrons that are excited by UV radiation but do not escape the surface of the grains will not heat the gas, they will on the other hand elevate the temperature of the grains themselves.

7.2.3 **Grain Irradiation**

Photons less energetic than UV photons will not ionize dust grains but will also heat them through excitation of electrons. Using a similar analysis as in the previous section we can write for the corresponding rate of heat deposition per volume

$$\Gamma_{\rm d} = 4\pi n_{\rm d}\sigma_{\rm d}\int_{\rm VIS} Q_{\nu,{\rm abs}} J_\nu\, d\nu, \tag{7.25}$$

where the integral is limited to optical photons and the absorption efficiency factor $Q_{\nu,{\rm abs}} \propto \nu$ in the visual band (see Chapter 2). We now express the mean intensity with the diluted $T \simeq 5{,}400$ K blackbody radiation discussed in Section 7.2 and Figure 7.1 to write

$$\begin{aligned}\Gamma_{\rm d} &\simeq 4\pi W n_{\rm d}\sigma_{\rm d} Q_{\nu,\max}\int_0^\infty \frac{\nu}{\nu_{\max}}\cdot\frac{2h\nu^3/c^2}{e^{h\nu/kT}-1}\,d\nu \\ &\simeq \frac{8\pi W n_{\rm d}\sigma_{\rm d} Q_{\nu,\max}k^5T^5}{h^4c^2\nu_{\max}}\int_0^\infty \frac{x^4}{e^x-1}\,dx,\end{aligned} \tag{7.26}$$

with $W = 10^{-13}$, $x \equiv h\nu/kT$, and $Q_{\nu,\mathrm{abs}} \equiv Q_{\nu,\max}\,\nu/\nu_{\max}$. Using equation (7.22), $Q_{\nu,\max} = 0.1$ for $\nu_{\max} = 3\times10^{14}$ Hz (corresponding to the optical maximum at $\log\nu = 14.5$ in Figure 7.1), as well as the necessary information from a good definite integral table we find that

$$\Gamma_{\mathrm{d}} = 2\times10^{-9}\left(\frac{n_{\mathrm{H}}}{10^{3}\ \mathrm{cm}^{-3}}\right)\ \mathrm{eV\ cm^{-3}s^{-1}}. \tag{7.27}$$

7.2.4 **Stellar X-rays**

The radiation from high-mass protostars within molecular clouds can also heat up the gas through the ionization of dust as explained in Section 7.2.2; the level of the UV field can exhibit an enhancement $G_{\circ} \approx 10^{6}$ in the vicinity of O and B stars. Likewise, the radiation emanating from low-mass, i.e., T-Tauri, protostars will be absorbed by dust grains by the irradiation process discussed in the previous section, since most of their radiation happens at near-infrared and optical wavelengths (again, the intensity must be scaled in relation to the mean interstellar radiation field to adapt equation (7.27)).

But T-Tauri stars also emit 1/10,000 of their total flux in the form of X-rays, originating from **thermal bremsstrahlung** radiation in plasmas at temperatures of approximately 10^{7} K (i.e, $kT \approx 1$ keV). These high-energy photons will mostly ionize atomic hydrogen and helium. The X-ray spectrum of a star will usually be fairly flat until some frequency ν_{X} beyond which it will quickly fall off. If we consider a star centered within a sphere of atomic hydrogen gas, then we can write the flux contained in a frequency interval $\Delta\nu$ at a given position r in the sphere as

$$F_{\nu}\Delta\nu = \frac{\Delta\nu}{\nu_{\max}}\frac{L_{\mathrm{X}}}{4\pi r^{2}}e^{-\tau_{\nu}}, \quad \nu \le \nu_{\mathrm{X}}, \tag{7.28}$$

where L_{X} is the X-ray luminosity of the star and $\tau_{\nu} = n_{\mathrm{H}}\sigma_{\nu}r$. The cross-section of hydrogen σ_{ν} at X-ray wavelengths is found to be proportional to ν^{3} and we therefore write $\sigma_{\nu} = \sigma_{\mathrm{X}}\left(\nu/\nu_{\mathrm{X}}\right)^{3}$. If every X-ray photon is absorbed and its energy entirely transformed into heat we can write for the rate of heat deposition per unit volume at r

$$\begin{aligned}\Gamma_{\mathrm{X}} &\simeq \int_{0}^{\nu_{\mathrm{X}}} n_{\mathrm{H}}\sigma_{\nu}F_{\nu}\,d\nu \\ &\simeq \frac{n_{\mathrm{H}}L_{\mathrm{X}}}{4\pi r^{2}\nu_{\mathrm{X}}}\int_{0}^{\nu_{\mathrm{X}}}\sigma_{\nu}e^{-\tau_{\nu}}\,d\nu.\end{aligned} \tag{7.29}$$

Since the radiation will be most ionizing at the highest frequency, we can see from equation (7.28) that flux will approximately disappear for $\tau_{\mathrm{X}} = n_{\mathrm{H}}\sigma_{\mathrm{X}}r \approx 1$ or at a radius

$$r_{\rm X} \equiv \left(n_{\rm H}\sigma_{\rm X}\right)^{-1}. \tag{7.30}$$

The cross-section of hydrogen is $\sigma_\nu = 2\times10^{-22}\,{\rm cm}^2$ for X-ray photons of 1 keV. Equation (7.29) can be approximated (with a Gaussian integrand!) to yield

$$\begin{aligned}\Gamma_{\rm X} &= \frac{1}{6e\sqrt{2\pi}}\frac{L_{\rm X}}{\tau_{\rm X}^{8/3}r_{\rm X}^3} \\ &= 2\times10^{-13}\left(\frac{n_{\rm H}}{10^3\ {\rm cm}^{-3}}\right)^{1/3}\left(\frac{L_{\rm X}}{10^{30}\ {\rm erg\ s}^{-1}}\right)\left(\frac{r}{0.1\ {\rm pc}}\right)^{-8/3}\ {\rm eV\ cm^{-3}s^{-1}},\end{aligned} \tag{7.31}$$

for $r < r_{\rm X}$.

7.3 Cooling by Atoms

In order to obtain some thermal balance in molecular clouds, the heating mechanisms previously described must be counter balanced by cooling processes. Since the gas is mostly composed of molecular hydrogen any heating cannot be effectively removed through emission from this molecule itself in most parts of molecular clouds where the level of excitation is not sufficient to bring about vibrational or other higher energy transitions. Rather, the numerous inelastic collisions that hydrogen will have with other components of the gas will transfer some of the energy provided through heating and lead to radiation from the colliding partners that will cool off the gas.

7.3.1 **Density Dependence**

Since the cooling can only happen after collisions take place, it is not surprising that the density of the gas will play a significant role in this process. As an example, we consider a two-level molecule, as we did in Chapter 6, and consider the effect of collisions on this molecule when embedded in a gas of density n (mostly that of hydrogen). Let us first focus on the case the gas density is much less than the critical density $n_{\rm crit}$ needed for this transition to significantly emit radiation. We recall from Section 5.4.1 that

$$n_{\rm crit} \equiv \frac{A_{\rm ul}}{\gamma_{\rm ul}}, \tag{7.32}$$

where the collision rate induced by the critical density is $\gamma_{\rm ul}n_{\rm crit}$ and the 'u' and 'l' subscripts denote the upper and lower levels, respectively. When $n \ll n_{\rm crit}$ basically every collisional excitation is soon followed by the spontaneous emission of a photon. The **cooling rate per unit volume** $\Lambda_{\rm ul}$ due to emission of photons then equals the collision rate per unit volume times ΔE the energy difference between the two levels. That is,

$$\begin{aligned}\Lambda_{\rm ul}\left(n \ll n_{\rm crit}\right) &= n_{\rm l} n \gamma_{\rm lu} \Delta E \\ &= \frac{g_{\rm u}}{g_{\rm l}} n_{\rm l} n \gamma_{\rm ul} \Delta E \, e^{-\Delta E/kT_{\rm kin}},\end{aligned} \tag{7.33}$$

where equation (6.22) was used to relate $\gamma_{\rm lu}$ and $\gamma_{\rm ul}$. Since the level of excitation through collisions is (by definition) small we can approximate $n_{\rm l} \simeq n$ and

$$\Lambda_{\rm ul}\left(n \ll n_{\rm crit}\right) \simeq \frac{g_{\rm u}}{g_{\rm l}} n^2 \gamma_{\rm ul} \Delta E \, e^{-\Delta E/kT_{\rm kin}}. \tag{7.34}$$

At the opposite limit when $n \gg n_{\rm crit}$ every collisional excitation is likely to be followed by a collisional de-excitation (as opposed to spontaneous emission). This implies that the two levels are in LTE and the cooling, still due to spontaneous emission from the upper state, is fixed by the equilibrium population levels with

$$\begin{aligned}\Lambda_{\rm ul}\left(n \gg n_{\rm crit}\right) &= n_{\rm u} A_{\rm ul} \Delta E \\ &= \frac{g_{\rm u}}{g_{\rm l}} n_{\rm l} A_{\rm ul} \Delta E \, e^{-\Delta E/kT_{\rm kin}}.\end{aligned} \tag{7.35}$$

Whatever the differences between the sub- and supercritical cases (i.e., equations (7.34) and (7.35)) it is found that the cooling rate per unit volume increases with density, as expected.

7.3.2 **Fine-Structure Spectral Line Splitting**

Although the main emission lines of atoms are not expected to be active in a cold environment, it is interesting that abundant species can still provide a significant amount of cooling. This is due to presence of the electron fine structure present in the spectra of atoms (see Sec. 5.2.1 in Chapter 5). Since the fine structure Hamiltonian mostly arises from the presence of electron spin-orbit coupling, it is necessary for atoms to have electronic orbitals populated for $n > 1$ (such that $l > 0$ is a possibility). Obviously, this will not be possible for hydrogen or helium in cold environment, as only the $n = 1$ orbital will be populated. We then have to look for possible fine-structure lines for the most abundant species, e.g., oxygen and carbon.

For an atom, the total angular momentum is given by

$$\mathbf{J} = \mathbf{L} + \mathbf{S} \tag{7.36}$$

with $\mathbf{L}$ and $\mathbf{S}$ the orbital and electron spin angular momenta respectively. The states are labeled accordingly with

$$^{(2S+1)}L_J \tag{7.37}$$

using the quantum numbers for the three angular momenta; $2S+1$ is called the **multiplicity**. The spin-orbit coupling is proportional to $\mathbf{L}\cdot\mathbf{S}$.

Neutral oxygen in its ground state has four electrons populating the 2p orbitals ($l=1$), which combine to yield $L=1$ and $S=1$. The possible values for the total angular momentum quantum number are therefore $J=0, 1, \text{and } 2$; the ground state is therefore found to be a **multiplet** of states with energies increasing from ${}^3P_2$ to ${}^3P_1$ to ${}^3P_0$. The ${}^3P_1 \rightarrow {}^3P_2$ occurs in the far-infrared at $63\ \mu\text{m}$ and therefore readily escapes for a wide range of densities (i.e., as long they are not too high) and provide an important amount of cooling. This transition corresponds to $\Delta E = 2.0\times10^{-2}\text{eV}$ or $T_0 = 230\ \text{K}$. This line, like every fine-structure lines, are all forbidden since they are **magnetic dipole transitions** (as opposed to electric dipole) and are denoted with brackets, as in $[\text{OI}]\ 63\ \mu\text{m}$, to make this apparent. For this particular transition the Einstein A coefficient is about 10^{-4}s^{-1}, and at a temperature on the order of 10 K the collisional de-excitation coefficient is $\gamma_{\text{ul}} \approx 10^{-11}\text{cm}^3\text{s}^{-1}$ (see Sec. 5.1) such that $n_{\text{crit}} \approx 10^6 - 10^7\,\text{cm}^{-3}$. Since the abundance of neutral oxygen relative to hydrogen is $\approx 4\times10^{-4}$ and the degeneracy for a given state is $2J+1$, we find that

$$\Lambda_{\text{OI}} = 2\times10^{-10}\left(\frac{n_{\text{H}}}{10^3\ \text{cm}^{-3}}\right)^2 e^{-230\ \text{K}/kT_{\text{kin}}}\ \text{eV cm}^{-3}\text{s}^{-1} \tag{7.38}$$

using equation (7.34).

Carbon will also bring cooling through fine-structure transitions, but in the regions where its abundance is most significant (in the envelopes of molecular clouds where it is not locked in CO) it is ionized through the process discussed in Section 7.2.1. In this case, CII has only one 2p electron with $L=1$, $S=1/2$, and $J=1/2$ and $3/2$. The ${}^2P_{3/2} \rightarrow {}^2P_{1/2}$ $[\text{CII}]\ 158\ \mu\text{m}$ forbidden magnetic dipole transition has $\Delta E = 7.93\times10^{-3}\text{eV}$ ($T_0 = 92\ \text{K}$), $\gamma_{\text{ul}} \approx 10^{-9}\text{cm}^3\text{s}^{-1}$ (it is an ion, see equation (5.10) in Sec. 5.1), and $A_{\text{ul}} = 2.4\times10^{-6}\text{s}^{-1}$. Once again using equation (7.34) we find

$$\Lambda_{\text{CII}} = 3\times10^{-9}\left(\frac{n_{\text{H}}}{10^3\ \text{cm}^{-3}}\right)^2 e^{-92\ \text{K}/kT_{\text{kin}}}\ \text{eV cm}^{-3}\text{s}^{-1}. \tag{7.39}$$

7.4 Cooling by Carbon Monoxide

Not surprisingly, the second most abundant molecule, ${}^{12}\text{C}{}^{16}\text{O}$ (hereafter CO), is the dominant molecular coolant in molecular clouds. We must be careful, however, and resist the temptation to blindly apply equation (7.35) since the strongest lines of CO are highly optically thick, which means that not all the photons resulting from rotational transitions will escape the molecular cloud. To analyze the problem we go back to equation (6.36) in Chapter 6, which we rewrite as

$$\begin{aligned}\tau_{J+1,J} &= \frac{c^3 N_{\rm CO} A_{J+1,J}}{16\pi\nu_{J+1,J}^3 \Delta V}\cdot\frac{g_{J+1}}{g_0}\cdot\frac{T_0(1\to 0)}{T_{\rm kin}} e^{-\Delta E_{J0}/kT_{\rm kin}}\left(1-e^{-\Delta E_{J+1,J}/kT_{\rm kin}}\right)\\ &= \tau_{10}\frac{A_{J+1,J}}{A_{10}}\cdot\frac{\nu_{10}^3}{\nu_{J+1,J}^3}\cdot\frac{g_{J+1}}{g_1}\cdot e^{-(\Delta E_{J0}-\Delta E_{10})/kT_{\rm kin}}\left(\frac{1-e^{-\Delta E_{J+1,J}/kT_{\rm kin}}}{1-e^{-\Delta E_{10}/kT_{\rm kin}}}\right),\end{aligned} \tag{7.40}$$

where $\Delta\nu_{J+1,J} = \nu_{J+1,J}\,\Delta V/c$. However, we also have that

$$\begin{aligned}A_{J+1,J} &\propto \left(\frac{J+1}{2J+3}\right)\nu_{J+1,J}^3\\ g_J &= 2J+1\\ \Delta E_{J0} &= \frac{\Delta E_{10}}{2}J(J+1)\end{aligned} \tag{7.41}$$

and then from equation (7.40)

$$\tau_{J+1,J} = \tau_{10} e^{-\Delta E_{10}(J+2)(J-1)/kT_{\rm kin}}\left(\frac{1-e^{-\Delta E_{10}(J+1)/kT_{\rm kin}}}{1-e^{-\Delta E_{10}/kT_{\rm kin}}}\right). \tag{7.42}$$

Although the optical depth of τ_{10} always extremely large ($\sim 10^3$), the presence of the lone exponential in equation (7.42) will quickly bring the optical depth close to unity at some relatively modest critical value J_* that can be numerically evaluated by setting $\tau_{J_*+1,J_*} = 1$ in this expression. The $J_*+1\to J_*$ transition is the first that will be marginally optically thick, i.e., higher transitions with $J > J_*$ will be optically thin and contributing less escaping radiation. On the other hand, transitions with $J < J_*$ will be so thick that their radiation will emanate from a smaller layer on the edge of the cloud; it follows that most of the total CO cooling will be due to the $J_*+1\to J_*$ transition.

We now use the first of equations (7.35) to evaluate the corresponding CO cooling rate per unit volume

$$\begin{aligned}\Lambda_{\rm CO}^* &= A_{J_*+1,J_*}\Delta E_{J_*+1,J_*} n_{\rm CO}\frac{g_{J_*+1}}{g_0 U} e^{-\Delta E_{J_*+1,0}/kT_{\rm kin}}\\ &\simeq \frac{3}{2}(J_*+1)^5\frac{(\Delta E_{10})^2}{kT_{\rm kin}} n_{\rm CO} A_{10} e^{-\Delta E_{10}(J_*+2)(J_*+1)/2kT_{\rm kin}}\\ &\simeq 5\times 10^{-12}\frac{(J_*+1)^5\,\Delta E_{10}}{kT_{\rm kin}} e^{-\Delta E_{10}(J_*+2)(J_*+1)/2kT_{\rm kin}}\left(\frac{n_{\rm H}}{10^3\ {\rm cm}^{-3}}\right)\ {\rm eV\ cm^{-3}s^{-1}},\end{aligned} \tag{7.43}$$

where we used equation (7.41), the proper abundance for CO ($\approx 10^{-4}$), and

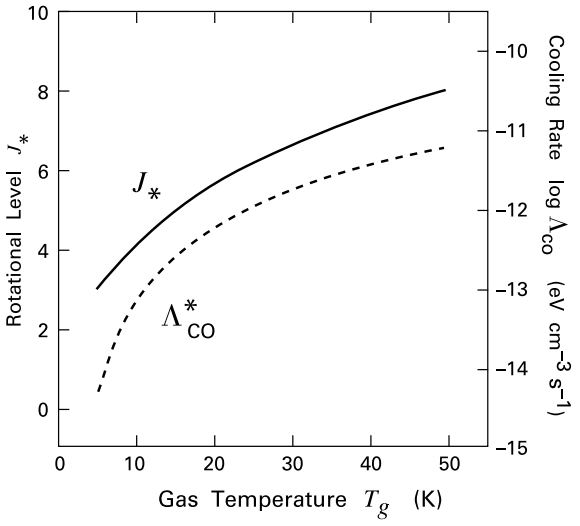

Figure 7.2 – Graph of J_* and the volumetric cooling rate $\Lambda^*_{\rm CO}$ as a function of the gas temperature $T_{\rm g} = T_{\rm kin}$.

$$n_{J_*+1} = n_{\rm CO}\frac{g_{J_*+1}}{g_0 U}e^{-\Delta E_{J_*+1,0}/kT_{\rm kin}}. \tag{7.44}$$

Figure 7.2 shows a plot of J_* and $\Lambda^*_{\rm CO}$ as a function of the kinetic temperature. A more accurate analysis seeking to evaluate the total CO cooling $\Lambda_{\rm CO}$ would need to include all transitions, especially those with $J < J_*$, which will be optically thick.

7.5 Thermal Effects of Dust

Dust grains are also efficient cooling agents as molecular clouds are optically thin to the radiation they emit at far-infrared wavelengths. To evaluate cooling rate per unit volume due to grains we take advantage of the fact that, as has been noted several times before, optical and UV radiation absorbed by grains will be processed and "re-emitted" at longer wavelengths; these incident and outgoing energies can therefore be equated under the assumption of equilibrium. We thus write

$$\Lambda_{\rm d} = 4\pi n_{\rm d}\sigma_{\rm d}\int_0^\infty Q_{\nu,\rm abs}B_\nu\left(T_{\rm d}\right)d\nu, \tag{7.45}$$

where it was assumed that the emission is isotropic (i.e., accounting for the "4π" factor), we set the absorption cross-section per unit volume to $n_{\rm d}\sigma_{\rm d}Q_{\nu,\rm abs}$, and emission can be suitably approximated with a blackbody function. In the far-infrared we can also model the absorption efficiency factor with (see Sec. 2.3)

$$Q_{\nu,\mathrm{abs}} = Q_{\nu,\max}\left(\frac{\nu}{\nu_{\max}}\right)^2, \tag{7.46}$$

and using equation (7.22) we rewrite the volumetric cooling rate as

$$\begin{aligned}\Lambda_{\mathrm{d}} &= \frac{4\pi Q_{\nu,\max}\Sigma_{\mathrm{d}} n_{\mathrm{H}}}{\nu_{\max}^2}\int_0^\infty \nu^2 B_\nu\left(T_{\mathrm{d}}\right)d\nu \\ &= \frac{4\pi Q_{\nu,\max}\Sigma_{\mathrm{d}} n_{\mathrm{H}} k^6 T_{\mathrm{d}}^6}{h^5 c^2 \nu_{\max}^2}\int_0^\infty \frac{x^5}{e^x-1}dx,\end{aligned} \tag{7.47}$$

with $x = h\nu/kT_{\mathrm{d}}$. Using adequate values for the different parameters, as well as solving for the integral, yields

$$\Lambda_{\mathrm{d}} = 1\times10^{-10}\left(\frac{n_{\mathrm{H}}}{10^3\ \mathrm{cm}^{-3}}\right)\left(\frac{T_{\mathrm{d}}}{10\ \mathrm{K}}\right)^6 \mathrm{eV\ cm^{-3}s^{-1}}. \tag{7.48}$$

Finally, the gas (i.e., H_2) will cool off due to collisions with the grain. This is because as a molecule, possessing a kinetic energy of $3kT_{\mathrm{kin}}/2$, hits a grain it will tend to stick to it for a long enough time to allow it to reach thermal equilibrium. Upon departing the surface of the grain its kinetic energy will therefore be $3kT_{\mathrm{d}}/2$ (note the different temperature), and the volumetric cooling rate (more precisely, the transfer of heat from the gas to the grain) will be

$$\begin{aligned}\Lambda_{\mathrm{g}\to\mathrm{d}} &= \frac{3}{2}k\left(T_{\mathrm{kin}}-T_{\mathrm{d}}\right)n_{\mathrm{d}}\nu_{\mathrm{c}} \\ &= \frac{3}{2}k\left(T_{\mathrm{kin}}-T_{\mathrm{d}}\right)n_{\mathrm{d}}n_{\mathrm{H}_2}v_{\mathrm{rel}}\sigma_{\mathrm{d}} \\ &= \frac{3}{4}k\left(T_{\mathrm{kin}}-T_{\mathrm{d}}\right)\Sigma_{\mathrm{d}}n_{\mathrm{H}}^2 v_{\mathrm{rel}} \\ &= 2\times10^{-14}\left(\frac{n_{\mathrm{H}}}{10^3\ \mathrm{cm}^{-3}}\right)^2\left(\frac{T_{\mathrm{kin}}}{10\ \mathrm{K}}\right)^{\frac{1}{2}}\left(\frac{T_{\mathrm{kin}}-T_{\mathrm{d}}}{10\ \mathrm{K}}\right)\mathrm{eV\ cm^{-3}s^{-1}},\end{aligned} \tag{7.49}$$

with ν_{c} the collision rate of hydrogen molecules with a grain and v_{rel} the average relative speed between colliding partners. We again emphasize that this process removes heat from the gas and deposit it in the dust grain population. That is, the energy extracted from the gas is not directly lost to interstellar space.

7.6 Summary of Heating and Cooling Processes

Table 7.1 - Heating and cooling processes

Process	Heating	Equation
Cosmic rays in HI	$p^+ + H \rightarrow H^+ + e^- + p^+$	(7.50)
Cosmic rays in H_2	$p^+ + H_2 \rightarrow H_2^+ + e^- + p^+$	(7.51)
Carbon ionization	$C + h\nu \rightarrow C^+ + e^-$	(7.52)
Photoelectric ejection (dust)		(7.53)
Dust irradiation		(7.54)
Stellar X-rays	$H + h\nu \rightarrow H^+ + e^-$	(7.55)

Process	Cooling	Equation
O collisional excitation	$O + H \rightarrow O + H + h\nu$	(7.56)
C^+ fine structure excitation	$C^+ + H \rightarrow C^+ + H + h\nu$	(7.57)
CO rotational excitation	$CO + H_2 \rightarrow CO + H_2 + h\nu$	(7.58)
Dust thermal emission		(7.59)
Gas-grain collision		(7.60)

The corresponding (and referenced) heating and cooling equations are given below.

7.6.1 **Volumetric Heating**

Cosmic rays in HI

$$\Gamma_{CR}(HI) = 1\times10^{-13}\left(\frac{n_{HI}}{10^3\ \mathrm{cm}^{-3}}\right)\ \mathrm{eV\ cm^{-3}s^{-1}}. \qquad (7.50)$$

Cosmic rays on H_2

$$\Gamma_{\rm CR}\left(\rm H_2\right) = 2\times10^{-13}\left(\frac{n_{\rm H_2}}{10^3\ \rm cm^{-3}}\right)\ \rm eV\ cm^{-3}s^{-1}. \tag{7.51}$$

Carbon ionization

$$\Gamma_{\rm CI} = 4\times10^{-11}\left(\frac{n_{\rm H}}{10^3\ \rm cm^{-3}}\right)\ \rm eV\ cm^{-3}s^{-1}. \tag{7.52}$$

Photoelectric ejection from dust

$$\Gamma_{\rm PE} = 3\times10^{-11}\left(\frac{n_{\rm H}}{10^3\ \rm cm^{-3}}\right)\ \rm eV\ cm^{-3}s^{-1}. \tag{7.53}$$

Dust irradiation

$$\Gamma_{\rm d} = 2\times10^{-9}\left(\frac{n_{\rm H}}{10^3\ \rm cm^{-3}}\right)\ \rm eV\ cm^{-3}s^{-1}, \tag{7.54}$$

which only heats up the dust grain population, not the (atomic/molecular) gas.

Stellar X-rays

$$\Gamma_{\rm X} = 2\times10^{-13}\left(\frac{n_{\rm H}}{10^3\ \rm cm^{-3}}\right)^{1/3}\left(\frac{L_{\rm X}}{10^{30}\ \rm erg\ s^{-1}}\right)\left(\frac{r}{0.1\ \rm pc}\right)^{-8/3}\ \rm eV\ cm^{-3}s^{-1}, \tag{7.55}$$

which only applies when the distance r from the stellar X-ray source is less than the maximum radial distance of penetration of the X-rays (i.e., $r < r_{\rm X}$).

7.6.2 **Volumetric Cooling**

O fine-structure excitation

$$\Lambda_{\rm OI} = 2\times10^{-10}\left(\frac{n_{\rm H}}{10^3\ \rm cm^{-3}}\right)^2 e^{-230\ \rm K/kT_{kin}}\ \rm eV\ cm^{-3}s^{-1}. \tag{7.56}$$

C^+ fine-structure excitation

$$\Lambda_{\rm CII} = 3\times10^{-9}\left(\frac{n_{\rm H}}{10^3\ \rm cm^{-3}}\right)^2 e^{-92\ \rm K/kT_{kin}}\ \rm eV\ cm^{-3}s^{-1}. \tag{7.57}$$

CO rotational excitation

$$\Lambda_{\rm CO}^{*} \simeq 5\times10^{-12}\,\frac{\left(J_{*}+1\right)^{5}\,\Delta E_{10}}{kT_{\rm kin}}\,e^{-\Delta E_{10}\left(J_{*}+2\right)\left(J_{*}+1\right)/2kT_{\rm kin}}\left(\frac{n_{\rm H}}{10^{3}\ {\rm cm}^{-3}}\right)\ {\rm eV\ cm^{-3}s^{-1}}, \qquad (7.58)$$

where J_{*} corresponds to the rotational transition $J_{*}+1\rightarrow J_{*}$ where the optical depth is close to unity.

Dust thermal emission

$$\Lambda_{\rm d} = 1\times10^{-10}\left(\frac{n_{\rm H}}{10^{3}\ {\rm cm}^{-3}}\right)\left(\frac{T_{\rm d}}{10\ {\rm K}}\right)^{6}\ {\rm eV\ cm^{-3}s^{-1}}. \qquad (7.59)$$

Gas-grain collisions

$$\Lambda_{\rm g\rightarrow d} = 2\times10^{-14}\left(\frac{n_{\rm H}}{10^{3}\ {\rm cm}^{-3}}\right)^{2}\left(\frac{T_{\rm kin}}{10\ {\rm K}}\right)^{1/2}\left(\frac{T_{\rm kin}-T_{\rm d}}{10\ {\rm K}}\right)\ {\rm eV\ cm^{-3}s^{-1}}, \qquad (7.60)$$

where this process removes heat from the gas and deposit it in the dust grain population. That is, the energy extracted from the gas is not directly lost to interstellar space.